The Influence of Soil Cave Diameter and the Thickness of the Overlying Clay Stratum on Ground Collapse in Karst Areas of Guangzhou

Weiqiang Liu[1], Jiayi Tian[2], Chunxi Ruan[1], Antai Yong[3], Yizhao Wang[4]
and Yan Gao[2*]

[1] Guangzhou Road Affairs Center, Guangzhou, 510630, China
[2] School of Earth Sciences and Engineering, Sun Yat-sen University, Zhuhai, 510082, China
[3] Guangzhou Transportation Bureau, Guangzhou, 510630, China
[4] Guangzhou Metro Design & Research Institute Co., Ltd., Guangzhou, 510010, China

*Corresponding author: gaoyan25@mail.sysu.edu.cn

Abstract. Utilizing field-measured engineering geological data, this study developed a finite element numerical model to simulate overlying clay stratum collapse in Guangzhou's karst terrain. The Euler-Lagrange coupling (CEL) technique was employed to dynamically replicate the evolutionary process of ground collapse. Following the orthogonal experimental design methodology, multiple numerical simulations were performed to quantify the sensitivity of key parameters to collapse magnitude and progression rate. By analyzing the propagation patterns of plastic zones and spatiotemporal variations in plastic strain, distinct evolutionary modes of overlying clay stratum collapse in karst regions were systematically categorized. Under low-intensity external disturbances, insufficient thickness of soil cave roofs triggers collapse, resulting in pronounced ground subsidence or sinkhole formation. Enlarged cave diameters amplify both the magnitude and velocity of collapse, whereas greater overlying clay stratum thickness suppresses these trends.

Keywords: Karst; collapse of overlying clay stratum; collapse characteristics

1   Introduction

In regions with unstable geological profiles and weak soil layers, ground deformation and subsequent collapse phenomena gradually manifest when subjected to external pressures, precipitation infiltration, or subsurface infrastructure leakage. Based on triggering mechanisms, ground collapses are categorized into two primary types: those linked to karst processes and those unrelated to karst activity. These events exhibit significant spatial clustering across China, with higher frequencies observed in northeastern, northwestern, northern, and southern provinces. Among them, karst collapses are more common in the south region, while mining-induced ground collapses are predom

reveal a tripartite classification: karst-induced collapses dominate (97.9%), followed by mining subsidence (0.8%) and miscellaneous forms (1.3%) [2]. The prevalence of karst geology in Guangzhou directly drives collapse mechanisms, as dissolution-induced fissures and cavities facilitate soil migration. Most events involve overburden failure above karst voids, while sporadic collapses stem from soluble bedrock roof instability.

The formative dynamics of soil cavities within clay-dominated karst overburdens are well-documented in existing literature. Baplov's subsurface erosion model and Xu et al.'s vacuum suction hypothesis [3] effectively describes particle migration and cavity propagation mechanisms in granular or low-strength soils [4]. Clay stratum failures predominantly follow a "soil cavity propagation" pattern. Previous studies have prioritized soil composition analysis, yet multifactorial interactions affecting collapse magnitude remain understudied, and systematic investigations into spatial scales are limited. his study adopts the Coupled Eulerian-Lagrangian (CEL) technique to precisely quantify soil displacement and stress fields during collapse events, while maintaining numerical stability under large-strain conditions [5]. Full-process simulations are conducted to rigorously analyse the roles of cavity diameter and overburden thickness in collapse progression.

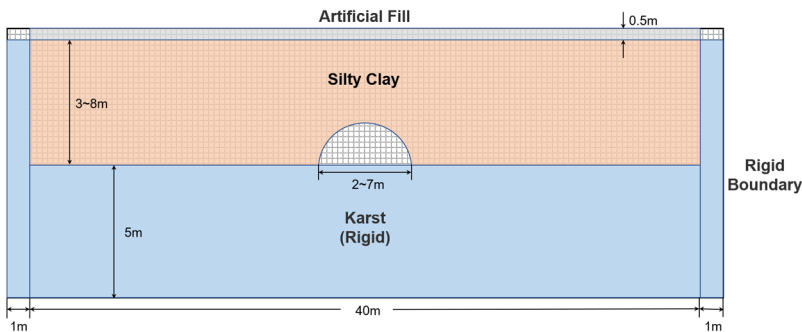## 2   Details of Numerical Simulations

Fig. 1. Schematic diagram of the model.

The clay stratum, extensively present in Guangzhou, constitutes roughly 46% of the Guanghua Basin's total area. In this research, ABAQUS-based finite element analysis was implemented to simulate collapse dynamics. Key model parameters include soil cavity diameter and overburden clay thickness, with the schematic configuration illustrated in Figure 1. The base layer comprises a 5 m-thick karst bedrock stratum, which exhibits negligible influence on overlying clay collapse and is thus modelled as a rigid boundary to optimize computational efficiency. A 0.5 m-thick artificial fill layer, representing surface engineering impacts, is superimposed with a gravitational load of 10 kPa. Its physical and mechanical properties—density (1960 kg/m^3), elastic modulus (26.6 MPa), and Poisson's ratio (0.3)—are assigned based on typical urban fill materials. The intermediate clay stratum, spanning 3–8 m in thickness, replicates the silty clay commonly encountered in Guangzhou's engineering projects. Material properties

include a density of 1840 kg/m^3, elastic modulus of 40.0 MPa, Poisson's ratio of 0.3, cohesion of 20 kPa, and internal friction angle of 13°. Given the high incidence of collapse at depths of 4–5m, the default overburden thickness above the soil cavity is fixed at 5 m. Soil cavity dimensions are calibrated to Guangzhou's field data: natural cohesive soil cavities typically range from 1 m to 3.5 m in height, corresponding to semicircular diameters of 2–7 m. Accordingly, the baseline cavity diameter is set to 5 m, with variations tested between 2 m and 7 m. To mitigate boundary interference, the model's horizontal span is defined as 40 m, flanked by 1 m-wide rigid constraints on both lateral edges. Soil yielding behavior is governed by the Mohr-Coulomb constitutive model.

3   Influence of Soil Cave Diameter

Numerical simulations were performed to analyze the influence of soil cavity diameter on collapse dynamics, with the overburden thickness fixed at 5 m and cavity diameters varying between 2 m and 7 m. The evolution of plastic zones in the clay stratum and associated ground displacements, as cavity dimensions increased, are depicted in Figures 2 and 3.

As shown in Figure 2, distinct collapse mechanisms emerge across different cavity scales. For cavities with smaller diameters (2–3 m), plastic strain development remains localized within the clay stratum, failing to propagate to the surface. Consequently, ground displacements are minimal, as illustrated in Figures 3a and 3b. When cavity diameters expand to intermediate ranges (4–5 m), the plastic zone fully penetrates the overburden, triggering significant strain accumulation and measurable surface displacements. Despite these effects, partial stabilization through soil arching prevents complete collapse (Figures 3c and 3d). In contrast, larger cavities (6–7 m) exhibit reduced arch thickness at the crown, leading to progressive destabilization of the overburden. This culminates in rapid displacement escalation and eventual catastrophic collapse (Figures 3e and 3f). Ground displacement profiles demonstrate Gaussian symmetry, with peak displacements centred at the cavity axis. Both displacement magnitude and collapse extent exhibit a direct correlation with cavity diameter, while the time required for plastic zone maturation and collapse initiation decreases proportionally.

To further quantify collapse dynamics, temporal variations in maximum displacement and collapse rate (defined as the acceleration of displacement prior to failure) are analyzed in Figure 4. Three distinct collapse modes are identified. For smaller cavities (2–3 m), collapse rates decay logarithmically over time, stabilizing at low displacement values. Intermediate cavities (4–5 m) display an initial surge in collapse rates followed by stabilization, corresponding to partial arch reinforcement. In larger cavities (6–7 m), collapse rates increase monotonically until abrupt structural breakdown occurs. The spatial extent of collapse, defined by surface displacements exceeding 200 mm, scales linearly with cavity diameter. The maximum influence range approximates 1.7 times the cavity diameter, indicating that collapse propagation requires cavity dimensions to surpass a critical threshold.
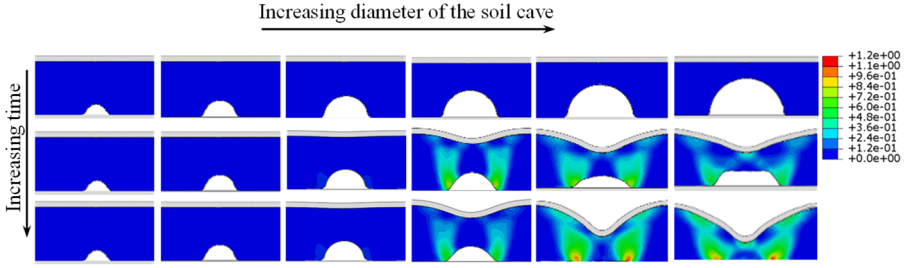
Fig. 2. The development of plastic zone during ground collapse process with increasing diameter of soil caves.
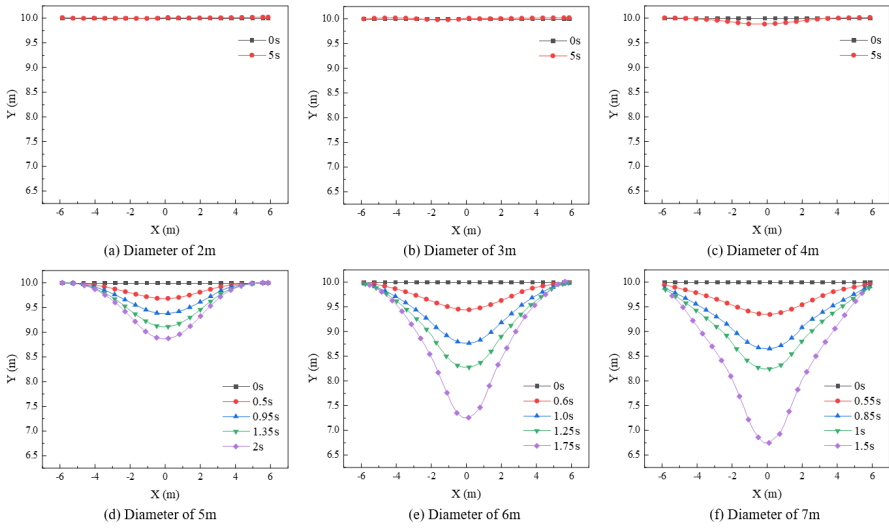

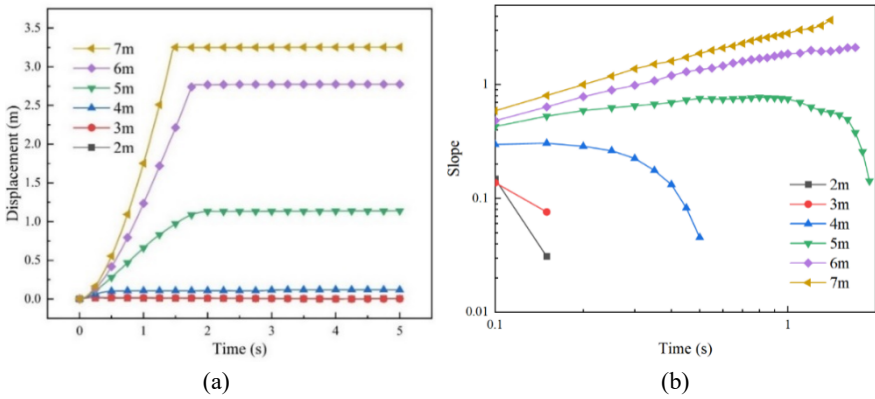**Fig. 3.** Ground displacement with increasing diameter of soil caves.

Fig. 4. Trend of maximum surface displacement and its changing rate with increasing diameter of soil cave: (a) maximum surface displacement; (b) collapse rate.

4   Thickness of Overlying Clay Stratum

To investigate the role of overburden thickness in ground collapse dynamics, simulations were conducted with a fixed cavity diameter of 5 m and clay stratum thickness varying between 3 m and 8 m. Analytical results reveal a Gaussian-symmetric ground displacement pattern centred at the cavity axis, consistent with observations from cavity diameter effects. Figure 5 illustrates the progression of plastic zones and temporal variations in maximum displacement and collapse rates. Notably, thicker clay strata correlate with reduced ground displacements but prolonged plastic zone development and collapse initiation times.
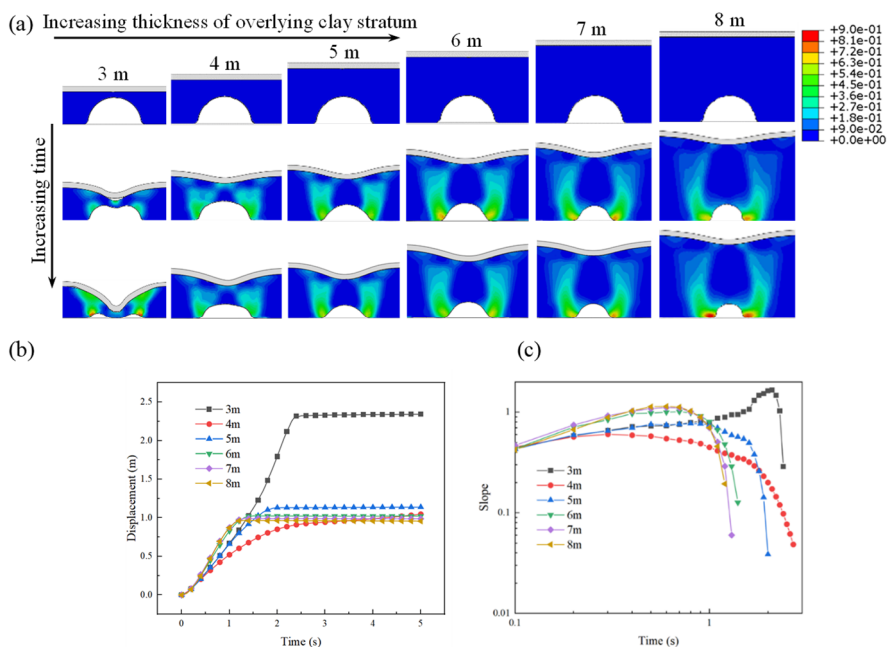

Fig. 5. Influence of the overlying clay stratum thickness on the maximum surface displacement: (a) plastic deformation evolution and collapse mechanisms (b) peak ground displacement; (c) failure progression rate

As shown in Figure 5a, the point of maximum plastic strain, which is approximately the point of soil arch failure, is farther away from the top of the soil arch with increasing thickness of the overlying clay stratum. Different stable arch shapes are also formed by different thicknesses of the clay stratum. Specifically, for smaller thicknesses of the clay stratum (less than or equal to 3 m), the height-to-span ratio of the stable arch is smaller, indicating a more flattened shape; the plastic zone within the clay stratum directly penetrates to the upper part, causing displacement and continuous increase of the clay stratum. Eventually, the upper soil collapses. In this case, the main triggering factor

for ground collapse is the excessive thinness of the roof of the cave. When the clay stratum is influenced by external loads, the cave continuously expands until the roof becomes unstable, leading to ground collapse. From an alternative perspective, based on the mechanical model conducted by Alonso et al [6], the formation of a stable soil arch requires a certain thickness of the stratum. This implies that the presence of an adequate overlying stratum is crucial for maintaining the stability of the soil arch. As the thickness of the clay stratum increases, the height-to-span ratio of the stable arch becomes larger (greater than 3 m), and the plastic zone within the clay stratum gradually penetrates in the whole soil and significant displacement is induced, however, a stable soil arch is finally formed with no soil cave collapse, in which only significant external loads can induce the ground collapse.

According to Figures 5b and 5c, the maximum ground displacement in the case of roof instability and collapse (with a clay stratum thickness of 3 m) is much larger than those in other cases. Apart from roof instability, as the thickness of overlying clay stratum increases, both the rate of collapse development and the extent of collapse tend to increase. With an increase in clay stratum thickness, the soil stabilizes in a shorter time under external influences. However, contrary to the commonly recognized conclusion that a thicker clay stratum leads to greater stability and reduces the likelihood of collapse, within a certain range, an increase in the thickness of the clay stratum results in greater gravitational forces, which in turn increases the plastic strain and the related horizontal influence range.
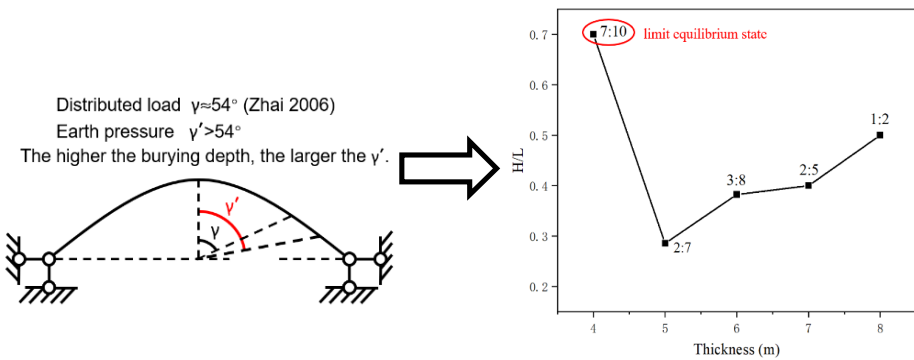

Fig. 6. The final shapes of the soil caves after ground deformation for different thicknesses of clay stratum.

Figure 5a demonstrates distinct variations in the final slope angles of soil cavities, dependent on overburden clay thickness. Plastic zone propagation followed inclined shear planes originating from cavity edges, as depicted in Figure 6. The measured average shear plane inclination (61°), partially supports Thigpen's theoretical framework [7], which posits a critical angle of $45 + \varphi/2$ where φ is the friction angle of the soil. Simulation and mechanical analyses in this study reveal that the critical slope angle is governed by both soil strength parameters and overburden thickness. Increasing overburden thickness initially reduces the cavity height-to-width ratio, followed by a marginal decline. A 1:2 ratio corresponds to the initial cavity geometry with negligible

deformation. Cavity geometry modifications are attributed to stress redistribution via soil arching mechanisms, enabling load transfer above the void [8-9]. Conventional analyses often idealize soil arches under uniform vertical loading [10-11]. However, non-uniform pressure distributions in real-world arches lead to critical angles deviating from Thigpen's predictions [7].

5   Conclusions

Through finite element numerical simulation, the scale of ground collapse for clay stratum overlying the karst are studied. It is found that the size of natural soil caves within a clay stratum overlying karst is the primary factor influencing both the degree and rate of ground collapse. Specifically, for every 1-meter increase of cave diameter, there is an associated increase in collapse rate and maximum surface displacement within ranges of 41.1~84.2% and 14.8~59.2%, respectively. While the thickness of the overlying clay stratum also impacts collapse rate within a range of 28.8~80.0%, its effect on the degree of collapse is relatively small at only 10.5~13.2%. Under minimal external influence, the natural soil cave in the clay stratum develops until it reaches its limit size. However, if the roof of the soil cave is too thin, the plastic zone may extend directly from the soil arch at the top to the ground surface, leading to plastic failure of the soil above the arch and subsequent instability, causing the soil to collapse into the cave, resulting in large-scale ground collapse or sinkholes, which is noticeably larger compared to other scenarios.

References

1. Zhang L F, Zeng X S, Yao Y S, et al. (2007) Review on karst collapse in China. Chin. J. Geol. Hazard Control., 18(3): 126-130. (in Chinese)
2. Lyu M N (2020) Analysis of ground settlement in Guangzhou city in recent years and countermeasures for prevention and control. Sci. Technol. Innov., (36): 137-138. (in Chinese)
3. Dong H G (2015) The formative environment and disaster - inducing factors of ground collapse disaster analysis in the Pearl River Delta of ground collapse. Geol. Miner. Resour. South China., 31(3):291 -296. (in Chinese)
4. Jiang F W (2017) Study on the developing model of karst collapse. Carsol. Sin., 36: 137-138.
5. Lin C H, Hung C and Hsu T Y (2020) Investigations of granular material behaviors using coupled Eulerian-Lagrangian technique: From granular collapse to fluid-structure interaction. Comput. Geotech., 121: 103485.
6. Alonso J, Moya M, Asensio L, et al (2022) A catenary model for the analysis of arching effect in soils and its application to predicting sinkhole collaps. Géotechnique., 72(6): 532-542.
7. Thigpen L (1984) Mechanics of strata collapse above underground openings. United States.
8. Protodyakonov M M (1907) Rock pressure on mine support (theory of mine support). Yekaterinoslav, Russia: Tipografiya Gubernskogo Zemstva (in Russian).

9. Chen Y M, Cao W P and Chen R P (2008) An experimental investigation of soil arching within basal reinforced and unreinforced piled embankments. Geotext. Geomembr., 26(2): 164-174.
10. Meng Y, Lei M T, Lin Y S, et al. (2012) Models and mechanisms of drilling-induced sinkhole in China. Environ Earth Sci., 67: 1961–1969.
11. Liu Z, Zhou C, Du Z, Su D, Li J and Zhang L (2018) Modeling cover-collapse sinkhole based on the theory of shells. Int. J. Comput. Mater. Sci. Eng., 8(1): 17.